Dynamic response of a scaled model of geosynthetic reinforced soil-integrated bridge system by shaking table test

C. Xu & M. Luo
Tongji University, Shanghai, China.

J. Han
University of Kansas, Lawrence, USA

ABSTRACT: Geosynthetic Reinforced Soil-Integrated Bridge System (GRS-IBS) is a new technology used for small to medium single-span bridges. At present, few studies have been done to investigate the response of GRS bridge abutments under dynamic loading conditions. In this paper, a complete bridge model with two GRS abutments and a bridge beam was designed and constructed for a model shaking table test to study the seismic performance of the GRS-IBS structure. A plane-strain scale model was designed using established similitude relationships for shaking table tests at 1g gravitational field. The GRS abutments were constructed using reinforcements, poorly-graded quartz sand, and modular facing blocks. The bridge beam was an aluminum plate and was placed on the GRS abutments at both ends. The reinforcement spacing of the two abutments was 0.05 m and 0.1 m respectively. A series of earthquake motions with different peak accelerations were applied to the model system in the longitudinal direction of the bridge beam. The acceleration responses, settlement of the bridge and displacement of GRS abutments were monitored. The residual settlement of bridge and lateral movement of abutments were small, which indicated good performance for the GRS-IBS under dynamic load.

1 INTRODUCTION

Geosynthetic Reinforced Soil (GRS) refers to alternating layers of highly compacted granular fill and closely-spaced (i.e., spacing no larger than 0.3 m) geosynthetic reinforcements (Adams et al. 2012). In recent years, GRS abutments have been increasingly used to support small to mid-span bridges due to the advantages of reduced construction cost, faster construction time, and effectiveness in eliminating bumps at the end of bridges (Keller and Devin 2003). Geosynthetic Reinforced Soil-Integrated Bridge System (GRS-IBS) is a refined development of GRS abutment in the construction details with the same advantages (Adams et al. 2007).

Many experimental and numerical investigations into bearing performance, deformation characteristics and mechanical properties of GRS abutments have been conducted under static loading conditions (Wu et al. 2013, Nicks et al. 2013, Adams et al. 2011, Saghebfar et al. 2017, Zheng & Fox, 2017). However, fewer studies investigate the seismic performance of GRS abutments for dynamic loading conditions. Helwany et al. (2012) carried out a large-scale shaking table test of the three-dimensional GRS abutment with a 3.6 m height, which was excited by a horizontal longitudinal sinusoidal wave. The test result showed that GRS abutment had good seismic performance. There was only 50 mm settlement at the surface and some local cracks at the bottom corner when the base peak acceleration was as high as 1.0 g. On the basis of this test, Helwany et al. (2012) also performed corresponding numerical analysis and the results were consistent with the test phenomena. Zheng et al. (2017, 2018) performed shaking table tests on a 2.7 m high half-scale GRS abutment with shaking in both the longitudinal and transverse directions, and observed only minor deformations after scaled earthquake motions with peak ground accelerations (PGA) of 0.31 g and 0.40 g.

From the preceding literature review, it can be concluded that fewer studies have been conducted to investigate the seismic response of GRS abutments under dynamic loading. In addition, all the shaking table tests of the GRS abutments reported in literature investigated the seismic performance of a single abutment with a segment of the bridge beam resting on top of it. The other end of the bridge beam segment was rested on a rigid support wall with rollers or a sliding platform (Helwany et al. 2012, Zheng et al. 2017, 2018). It should be noted that the use of the support wall may not reflect the true condition of the GRS abutments constructed in the field since the vertical fixity on top of the support wall did not allow the bridge beam to deform vertically. The vertical deflection of the bridge beam was important to the evaluation of differential settlement between the bridge and

the approach roadway and may affect the overall performance of the whole GRS-IBS system. Therefore, further studies may be necessary.

Based on the previous study of the shaking table test of the GRS abutment, this study designed and constructed a complete bridge model with two GRS abutments and a bridge beam for a shaking table test to study the seismic performance of the GRS-IBS structure.

2 TEST MODEL

2.1 *Similitude relationship*

The prototype was selected from the Guthrie Run Bridge in Delaware, USA, which is a typical GRS-IBS structure with a 6.0 m total height (Talebi 2016). Due to the limitations of the size of vibration table, the test model needed to be scaled by similarity ratio. Table 1 shows the similitude relationship used in this test, which was proposed by Iai (1989) and widely used for shaking table tests in a 1g gravitational field (El-Emam & Bathurst 2007, Guler & Selek 2014).

Table 1. Similitude relationships for 1g shaking table testing

Variable	Theoretical Scaling Factor (Iai 1989)	Scaling Factor in this Test ($\lambda = 4$)
Length	λ	4
Density	1	1
Stress	λ	4
Strain	1	1
Modulus	λ	4
Stiffness	λ^2	16
Time	$\lambda^{1/2}$	2
Frequency	$\lambda^{-1/2}$	1/2
Acceleration	1	1

2.2 *Model configuration*

The model test conducted in this study simulated a GRS abutment in a plane-strain condition. Figure 1 presents the configuration and geometry of the test model. The GRS-IBS model was constructed inside a test box with a net width of 0.7 m made of reinforced steel, including two GRS abutments and a bridge beam. The total length of the model structure was 4.0 m, of which the abutment on each side was approximately 1.3 m long. Therefore, the net span of the bridge beam between the two abutments was 1.4 m. The total height of the model structure was 1.5 m, of which the abutment height (H_a) was 1.2 m, the foundation thickness was 0.15 m and the approach thickness was 0.15 m. The bridge beam had dimensions of 2.1 × 0.68 × 0.15 m (length × width × thickness) and was placed directly on the GRS abutments at both ends. The bearing width for the bridge beam was 0.25 m and the setback distance between the back of the facing wall and the beam seat was zero. The clear space, defined as the distance from the top of the facing wall to the bottom of the bridge beam, was 0.05 m.

The layouts of the reinforcements for abutments on the two sides were different. Although the lengths of the reinforcements (L_r) in each abutment were all 0.84 m (i.e., $L_r = 0.7\ H_a$), the reinforcement spacing of left abutment was 0.1m while the right was 0.05 m. It should be noted, the right abutment was the reference group for this test, which was scaled strictly from engineering prototype according to the similitude relationships showed in Table 1. In addition, the reinforcement spacing of the reinforced soil foundation (wrapped layers) and the integrated approach (wrapped layers) were both 0.05 m.

The model abutment was limited by the test box on three sides and free on one side. The free side was a modular block facing wall in front of the model abutment, while Expanded Polystyrene (EPS) panel with a 0.05 m thickness was used for vibration reduction at the back wall of the test box to minimize boundary effects on the seismic response of the abutment. One side wall of the test box was a transparent Plexiglas panel for observation during testing.

2.3 *Material*

The backfill soil for this study was a poorly-graded quartz sand with a coefficient of uniformity $C_u = 2$, and a coefficient of curvature $C_c = 0.95$. The maximum and the minimum dry density were 1.74 g/cm^3 and 1.33 g/cm^3 respectively. During construction, the sand was compacted to reach the dry density of 1.64 g/cm^3, which corresponded to a relative density of approximately 80 %. According to the triaxial test, the sand had an internal friction angle of 49º and zero cohesion when the relative density was 80 %.

The reinforcement for this study was a biaxial low-intensity geogrid made of polyethylene which was carefully selected to meet the scaling requirements in Table 1. The aperture sizes of the geogrids were 33 × 33 mm. The rib width and thickness of the geogrids were 3.5 mm and 1.0 mm respectively. Due to the different reinforcement spacing between two abutments, half of the ribs of the geogrids used in the right abutment were cut to keep the ratio of the reinforcement stiffness to the reinforcement spacing constant. The main mechanical properties of geogrids are presented in Table 2.

The bridge beam was an aluminum plate with the dimensions of 2.1 × 0.68 × 0.15 m as mentioned earlier, which weighed about 0.65 tons and could apply a uniform load of 18.3 kPa to each abutment. This applied load on the abutment just satisfied the scaling requirement without considering the live loads caused by the vehicle. The modular block of the facing wall was a brick with the dimensions of 0.23 × 0.1 × 0.05 m (length × width × thickness).

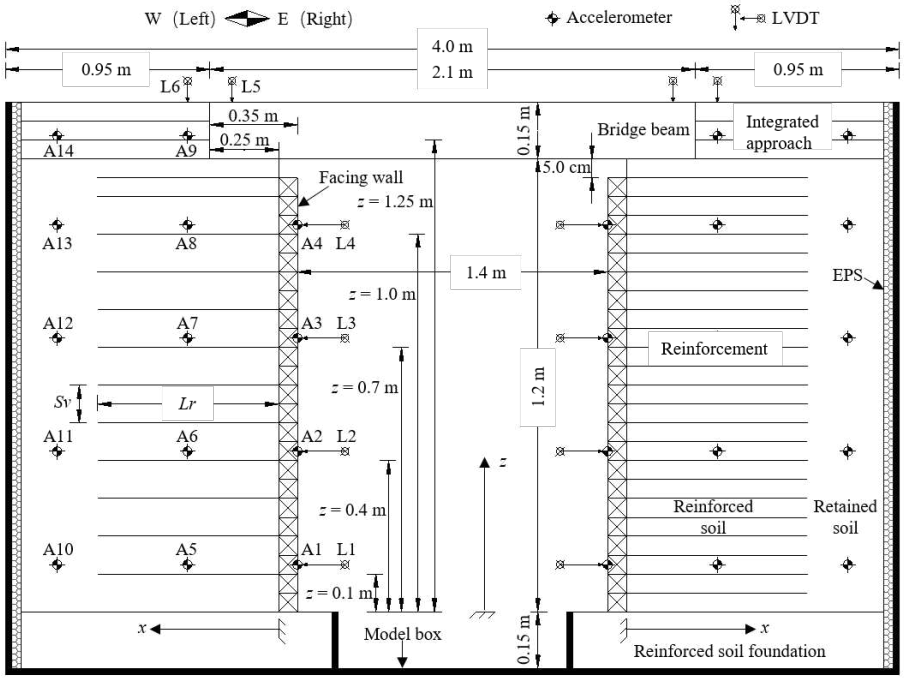

Note: The serial number of the monitoring instruments of the right abutment is the same as that of the left abutment in a symmetrical position

Figure 1. The configuration and geometry of test model and instrumentation for centerline section in longitudinal direction

Table 2. The main mechanical properties of geogrids

Property	Left abutment	Right abutment
Ultimate tensile strength (kN/m)	10	5
Tensile strength at 2% tensile strain (kN/m)	3.4	1.6
Tensile stiffness at 2% tensile strain (kN/m)	170	80

2.4 *Construction*

A 0.15-m-thick reinforced soil foundation was first placed at the bottom of the test box with a relative density of 80%. in order to provide a firm base for the GRS abutment. The abutment was then built in the order of "laying a row of blocks - laying a layer of backfill - laying a layer of reinforcement" until the design height. The layer thickness was 0.05 m and there were 24 layers of each GRS abutment. The third step was to install the bridge beam gently and the last step was to construct the integrated approach.

The backfill was compacted to reach the required relative density of 80 % in each layer by a hand-held plate vibrator with a power of 390 W. The modular blocks were stacked layer by layer, and a running bond was maintained between courses of block so that the joints between the blocks were offset with each row. Additionally, each layer of modular blocks should be placed horizontally, and each block should be placed tightly against the adjoining block for preventing gaps from which backfill soil could escape. The geogrids were tied by lead wire one layer by one layer to achieve the mechanical connection.

Some measures to reduce friction were applied on both sides of the test box to ensure the plane strain condition. A lubrication layer consisted of a 0.4-mm-thick polytetrafluoroethylene membrane and an approximately 1.0-mm-thick Vaseline was created on the inside surface of the steel plate. On the other hand, a layer of silicone oil was brushed directly on the inside surface of the Plexiglas panel.

2.5 *Instrumentation*

The acceleration responses, settlement of the bridge and displacement of GRS abutments were monitored. The accelerometers for accelerations and linear variable differential transducers (LVDTs) for lateral facing displacements and bridge beam settlements were instrumented for the longitudinal section at the centerline as shown in Figure 1.

3 INPUT MOTIONS

A series of horizontal motions, including white noise motions and scaled earthquake motion, were applied to the GRS-IBS structure in the longitudinal direction. Figure 2 shows the time histories of the scaled Kobe earthquake motion with a peak ground acceleration (PGA) of 1.0 g which was used as a horizontal excitation. The original earthquake motion was recorded by the Japan Meteorological Agency during the Kobe earthquake, and the North-South (N-S) component of the earthquake records was used in this test. The white noise motions were used to characterize natural frequencies of the model system and identify any changes in system response before and after the excitation by scaled Kobe earthquake motion. The nominal white noise motion had a peak acceleration of 0.05 g and frequency content ranging from 0.1 Hz to 50 Hz. It should be noted that the positive direction of Kobe motion corresponded to the west (i.e., the left side of the GRS-IBS structure which was marked in

Figure 1), and the interval between each excitation was 5 min.

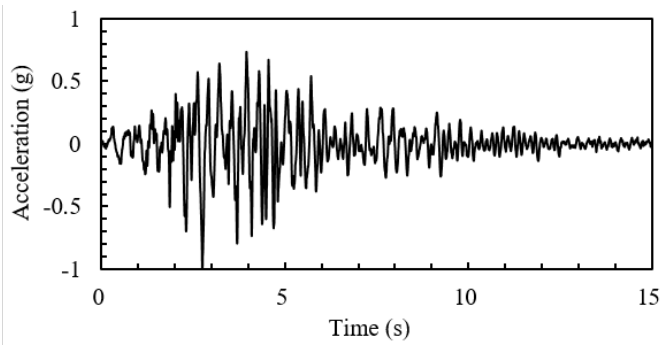

Figure 2. The time histories of Kobe earthquake motion

4 RESULTS

4.1 *Acceleration response*

A detailed description of the test results is not possible due to limited space, as an example, Figure 3 shows the measured acceleration time histories of the facing wall of the abutments at four selected elevations. From Figure 3, we find out the measured positive acceleration amplitudes of the left abutment were generally larger than those in the right abutment due to the asymmetry of input Kobe motion and the opposite outward directions of the left and right GRS abutment facing. Figure 4 further illustrates the same result drawn from Figure 3.

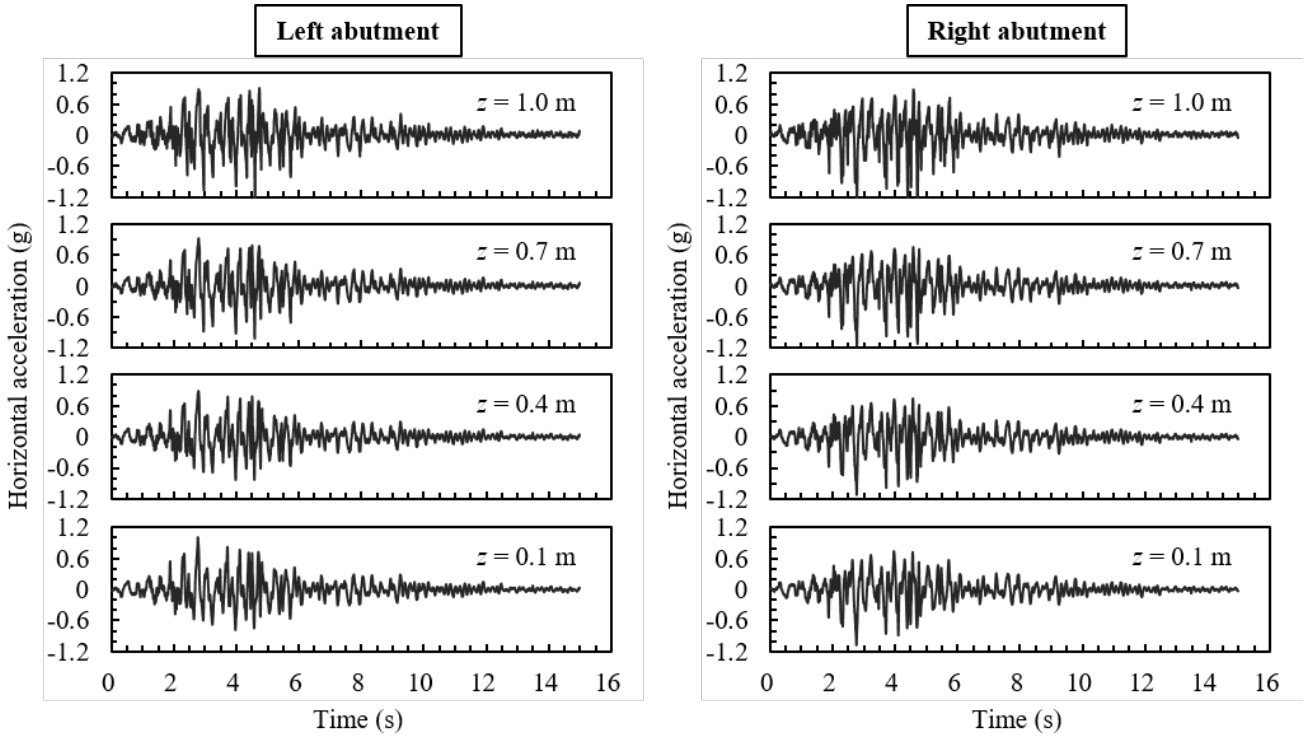

Figure 3. Time histories of response acceleration for facing wall.

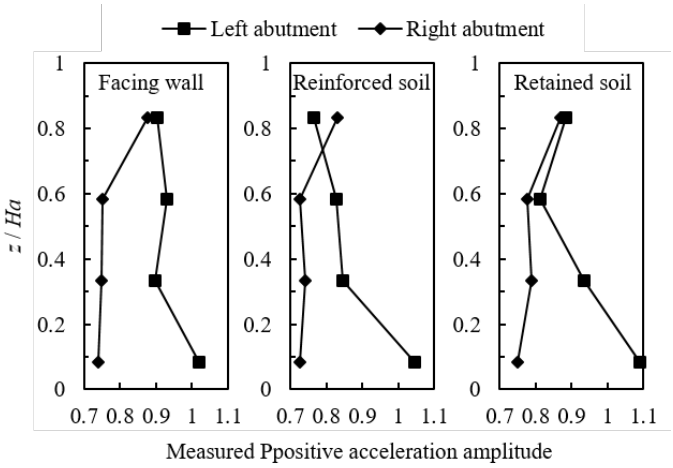

Figure 4. The measured positive acceleration amplitudes of the left and right abutments at selected elevations

Figure 5 shows the peak acceleration amplification ratio profiles for the facing, reinforced soil and retained soil in the abutments. The results indicate that the peak acceleration amplification ratio increases with elevation in the right abutment, while decreases with elevation in the left abutment. This may be due to the asymmetry and directionality of the Kobe motion. The peak acceleration amplification ratios of the facing and retained soil are slightly larger than that of the reinforced soil. In general, the peak acceleration amplification ratios are relatively small and the largest ratio is just 1.2 near the top of wall facing, which is likely due to the closely reinforcement spacing for providing sufficient lateral restraint to the GRS abutment.

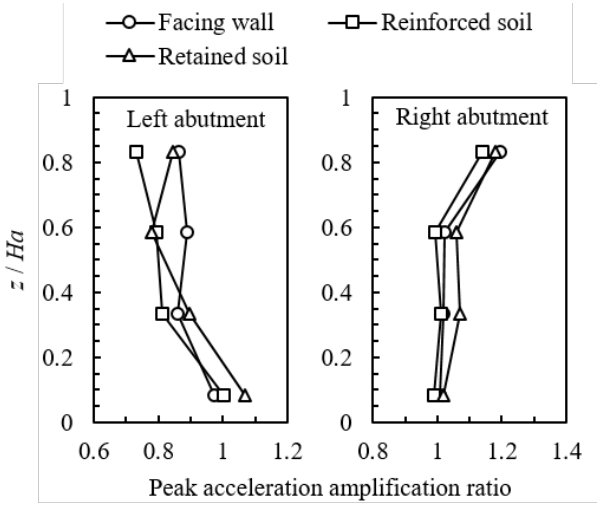

Figure 5. Peak acceleration amplification ratio profiles in the GRS abutments

4.2 *Lateral displacement and vertical settlement*

Figure 6 shows the permanent lateral displacement distributions of the GRS abutments after the termination of the experiment, when the peak ground acceleration of the input motion has reached to 1.0 g. In Figure 6, the instrument measurements at the centerline of the facing wall are compared to the manual measurements on the both sides of the facing wall. The results are relatively close; this proves that the result monitored by the instrument is reliable. In addition, it can be found that the lateral displacements of the left abutment are much larger than the lateral displacements of the right abutment. The possible reason is that the reinforcement spacing of the right abutment is small, which results in a greater restriction on lateral deformation. On the other hand, the measured positive acceleration amplitudes of the left abutment was much larger than that of the right abutment as shown in Figure 3 and Figure 4, and this would also cause the lateral displacement of the left abutment to be greater than the lateral displacement of the right abutment. However, in general, the lateral displacements of the abutments did not exceed 30 mm (i.e., the deformation of the abutment did not exceed 2.5%). This indicated good seismic performance for the GRS-IBS structure and there was only a small deformation under strong earthquake motion.

Table 3 gives the final settlement at the end of bridge beam and the differential settlement between the bridge beam and the integrated approach. It can be seen from Table 3 that the settlement and differential settlement are very small. This further illustrates that the GRS-IBS structure has good seismic performance.

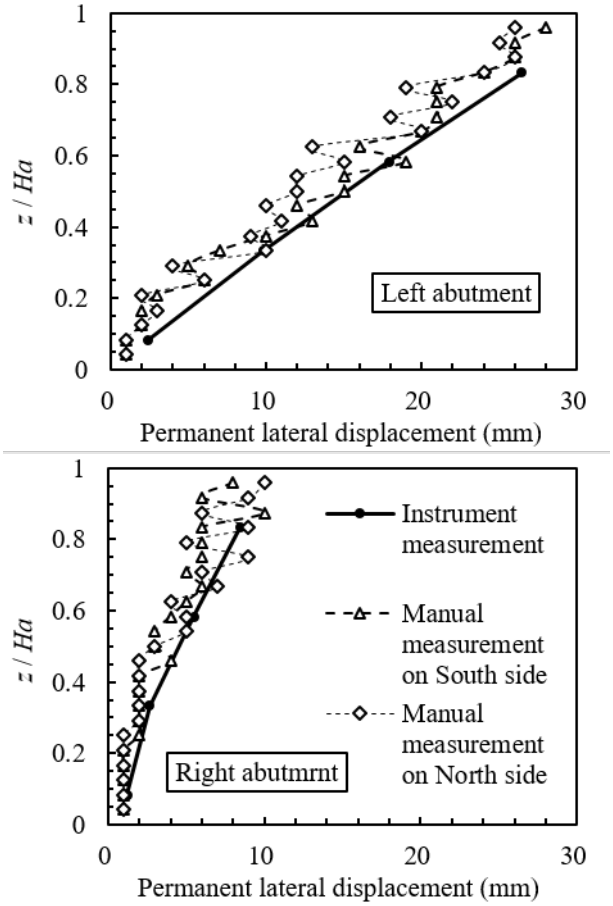

Figure 6. The distribution of permanent lateral displacement

Table 3. Settlement and differential settlement after the termination of the test

Monitoring program	Location	
	Left abutment	Right abutment
Settlement (mm)	5.0	3.0
Differential settlement (mm)	1.5	1.0

5 CONCLUSIONS

This paper detailed the design and construction of a scaled GRS-IBS model for a shaking table test. A preliminary analysis of the test results was conducted.

This paper presented the acceleration responses of the right abutment (including the bridge beam and the integrated approach) for a peak ground acceleration of 1.0 g with a duration of 15 seconds as an example. The results indicated that the peak acceleration amplification ratios are relatively small in general and the largest ratio is just 1.2 in the GRS abutment meaning the seismic performance of this structure is good.

The lateral displacement of abutments, settlement at the end of bridge beam and the differential settlement between the bridge beam and the integrated approach were monitored. The results showed that the residual settlement of bridge beam and lateral displacement of abutments were small.

6 ACKNOWLEDGEMENTS

This study was financially supported by the Key Research and Development Project of Chinese Ministry of Science and Technology (Grant No. 2016YFE0105800). The authors would like to acknowledge this support.

7 REFERENCES

Adams, M.T. Nicks, J. Stabile, T. Wu, J.T.H. Schlatter, W. & Hartmann, J. 2012. *Geosynthetic Reinforced Soil Integrated Bridge System Interim Implementation Guide*, Report No., FHWA-HRT-11-026, the US Federal Highway Administration, McLean, VA, USA.

Adams, M.T. Schlatter, W. & Stabile, T. 2007. Geosynthetic Reinforced Soil Integrated Abutments at the Bowman Road Bridge in Defiance County, Ohio. *Proceedings of Geo-Denver 2007: Geosynthetics in Reinforcement and Hydraulic Applications, Geotechnical special publication 165*, ASCE, Reston, VA, USA: 16-26.

Adams, M.T. Nicks, J. Stabile, T. Wu, J.T.H. Schlatter, W. & Hartmann, J. 2011. *Geosynthetic reinforced soil integrated bridge system synthesis report*, Report No., FHWA-HRT-11-027, the US Federal Highway Administration, McLean, VA, USA.

El-Emam, M. & Bathurst, R.J. 2007. Influence of reinforcement parameters on the seismic response of reduced-scale reinforced soil retaining walls. *Geotextiles and Geomembranes*, 25(1): 33-49.

Guler, E. & Selek, O. 2014. Reduced-scale shaking table tests on geosynthetic-reinforced soil walls with modular facing. *Journal of Geotechnical and Geoenvironmental Engineering*, 140(6): 04014015.

Helwany, S.M.B. Wu, J.T.H. & Meinholz, P. 2012. *Seismic Design of Geosynthetic-Reinforced Soil Bridge Abutments with Modular Block Facing*, NCHRP Web-Only Document 187, Transportation Research Board, Washington, DC, USA.

Iai, S. 1989. Similitude for shaking table tests on soil-structure-fluid models in 1 g gravitational fields. *Soils and Foundations*. 29(1): 105-118.

Keller, G, & Devin, S. 2003. Geosynthetic-Reinforced Soil Bridge Abutments. *Transportation Research Record: Journal of the Transportation Research Board*, 1819: 362-368.

Nicks, J.E. Adams, M.T. Ooi, P.S.K & Stabile, T. 2013. *Geosynthetic reinforced soil performance testing – Axial loading deformation relationship*, Report No., FHWA-HRT-13-066, the US Federal Highway Administration, McLean, VA, USA.

Saghebfar, M. Abu-Farsakh, M. Ardah, A. Chen, Q. & Fernandez, B.A. 2017. Performance monitoring of Geosynthetic Reinforced Soil Integrated Bridge System (GRS-IBS) in Louisiana, *Geotextiles and Geomembranes*. 45(2): 34-47.

Talebi, M. *Analysis of the Field Behavior of a Geosynthetic Reinforced Soil Integrated Bridge System During Construction and Operation*, The university of Delaware, 2016.

Wu, J.T.H. Pham, T.Q. & Adams, M.T. 2013. *Composite Behavior of Geosynthetic Reinforced Soil Mass*. Report No. FHWA-HRT-10-077, the US Federal Highway Administration, McLean, VA, USA.

Zheng, Y. & Fox, P.J. 2017. Numerical investigation of the geosynthetic reinforced soil-integrated bridge system under static loading, *Journal of Geotechnical and Geoenvironmental Engineering.* 143(6): 1-14.

Zheng, Y. Sander, A.C. Rong, W. Fox, P.J. Shing, P.B. & McCartney, J.S. 2017. Shaking Table Test of a Half-Scale Geosynthetic-Reinforced Soil Bridge Abutment, *Geotechnical Testing Journal*. 41(1): 20160268.

Zheng, Y. McCartney, J.S. Shing, P.B. and Fox, P.J. 2018. Transverse shaking table test of a half-scale geosynthetic reinforced soil bridge abutment, *Geosynthetics International*. 25(6): 582-598.